IEEE Photonics Journal
An IEEE Photonics Society Publication

Open Access

An SVM-Based Detection for Coherent Optical APSK Systems With Nonlinear Phase Noise

Volume 6, Number 5, October 2014

Yi Han
Song Yu
Minliang Li
Jie Yang
Wanyi Gu

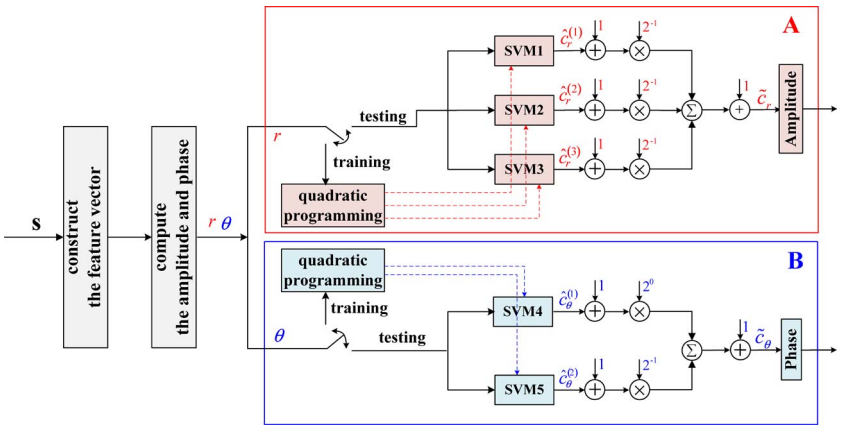

DOI: 10.1109/JPHOT.2014.2357424
1943-0655

An SVM-Based Detection for Coherent Optical APSK Systems With Nonlinear Phase Noise

Yi Han, Song Yu, Minliang Li, Jie Yang, and Wanyi Gu

State Key Laboratory of Information Photonics and Optical Communications, Beijing University of Posts and Telecommunications, Beijing 100876, China

DOI: 10.1109/JPHOT.2014.2357424

Manuscript received August 30, 2014; accepted September 6, 2014. Date of publication September 12, 2014; date of current version October 13, 2014. This work was supported in part by the National Basic Research Program of China (973 Program) under Grant 2012CB315605 and Grant 2014CB340102, by the National Natural Science Foundation under Grant 61271191 and Grant 61271193, by the Fund of the State Key Laboratory of Information Photonics and Optical Communications, and by the Fundamental Research Funds for the Central Universities. Corresponding author: S. Yu (e-mail: yusong@bupt.edu.cn).

Abstract: A support vector machine (SVM)-based data detection is proposed for coherent optical fiber amplitude phase-shift keying (APSK) communication systems where the nonlinear phase noise is the main system impairment. The performances of the detection with SVMs are investigated for three different 16-APSK modulation formats. In addition, three transmission scenarios with dispersion being considered or not are adopted to simulate and analyze the performances. Compared with the traditional two-stage maximum-likelihood detection, the SVM conducts detection without the need to know the information of transmission link, and it gains a relatively large improvement in the nonlinear system tolerance, particularly in the high nonlinear regime. Compared with quadrature amplitude modulation (QAM), the 16-APSK system can increase the nonlinear system tolerance by 4.88 dB at BER $= 1E-3$.

Index Terms: Support vector machine (SVM), amplitude phase-shift keying (APSK), nonlinear phase noise (NLPN).

1. Introduction

In order to expand the capacity of optical fiber communication systems, the improvement of the spectral efficiency has been a concern in recent years [1]. Higher order Quadrature Amplitude Modulation (QAM) with coherent detection is considered as an effective way to achieve high spectral efficiency, which encodes information on all available degrees of freedom [2]. While the more densely packed constellation endows systems with higher spectral efficiency, it is more sensitive to channel impairments. Among the fiber-induced impairments, nonlinear phase noise (NLPN) is a primary obstacle and severely limits the transmission distance as well as the capacity [3]. Various approaches have been investigated for combating the effect of NLPN in optical QAM systems, e.g., phase pre- [4] and post-compensation [5] in electric field, the maximum likelihood (ML) detector [6], maximum likelihood sequence estimation (MLSE) [7] and M-ary support vector machine (SVM) [8].

However, due to the characteristic of the constellation, the QAM signals are very sensitive to phase noise especially the NLPN [9], and their performances degenerate severely during

transmission in optical fiber systems. Consequently, the amplitude phase shift keying (APSK) constellation has received considerable attention for the improvement of the fiber nonlinear tolerance [10]. The amplitude and phase distribution of APSK constellations can be adjusted suitably to overcome the defect of the QAM constellations. To benefit more from APSK formats, the effect of NLPN must be minimized to upgrade the performance of coherent optical APSK systems.

To mitigate NLPN in coherent APSK systems, two stage (TS) ML detection in [11] has been used, which consists of radius detection, an amplitude-dependent phase compensation and phase detection. And by using the TS detection, some efforts have been devoted to the optimization of the APSK constellation so as to improve the nonlinear phase noise tolerance. For example, [12] has used the TS detector to optimize the 16-APSK constellation to achieve 2 dB performance gain in the nonlinear regime. In [13], four, eight, and 16 point constellations have been designed by minimizing the symbol error rate (SER) theoretically according to the improved TS detector. While the TS detector simplifies the optimization of constellations, it performs poorly in the high nonlinear regimes [14] for APSK systems. What's more, this suboptimal detection strategy requires a precise knowledge of the transmission link.

In this paper, SVM is applied as a detection scheme to mitigate the NLPN for coherent optical fiber APSK systems. Based on the received symbols rather than the probability density function (PDF) in theory, the SVM can generate optimum decision hyperplane which classifies the data more precisely. To study the performance of the detection scheme with SVMs, we specify the 16-points APSK constellations with three different modulation formats: (4444)-APSK, (484)-APSK, (88)-APSK. The performances of the three APSK systems using detection with SVMs are compared with that using the TS detector, respectively. To begin with, we consider the dispersion shift fiber (DSF) and focus on the NLPN. Then we move to the dispersion managed and unmanaged link to evaluate the performance of SVMs briefly. Since 16-QAM has been widely used in optical systems, a comparison with 16-QAM is also carried out through simulation. Various results indicate that using the detection scheme with SVMs can gain a significant improvement over the TS detector. For example, in the (88)-APSK system with DSF link, the nonlinear tolerance and the maximum distance at the BER $= 1E-3$ are increased by 1.8 dB and 11.5%, respectively. Furthermore compared to 16-QAM, the optimal nonlinear tolerance of the constructed 16-APSK can be improved by 4.88 dB.

Our paper is organized as follows. In Section 2, we introduce three conventional 16-APSK modulation formats and select appropriate bits mapping for them. Section 3 proposes a new NLPN mitigation technique by using SVMs for coherent optical APSK systems. The simulation model and results are given in Section 4. Finally concluding remarks and future work can be found in Section 5.

2. Construction of APSK Constellations

Generally, M-APSK constellation can be regarded as a union of N concentric rings, each with uniformly spaced phase-shift keying (PSK) points. In addition, the set of the signal constellation points is defined as [15]

$$\chi \triangleq \left\{ r_k \exp\left(j\frac{2\pi i}{I_k} + j\varphi_k \right) : 1 \le k \le N, 0 \le i \le I_k - 1 \right\} \tag{1}$$

where N denotes the number of amplitude rings, r_k is the radius of the kth ring, I_k is the number of points on the kth ring, and the sum of I_k satisfies $\sum_{k=1}^{N} I_k = M$, where φ_k is the phase offset in the kth ring. We assume a uniform distribution on the channel input signal over all symbols, then the average transmitted power $P_t = 1/M \sum_{k=1}^{N} I_k r_k^2$. In addition, the radii are ordered so that $r_1 < r_2 < \cdots < r_N$. In order to apply the SVM detector to the M-APSK systems, we focus on constellations with $M = 16$ and aim at several conventional 16-APSK modulation formats in this paper, namely (4444)-APSK, (88)-APSK, and (484)-APSK.

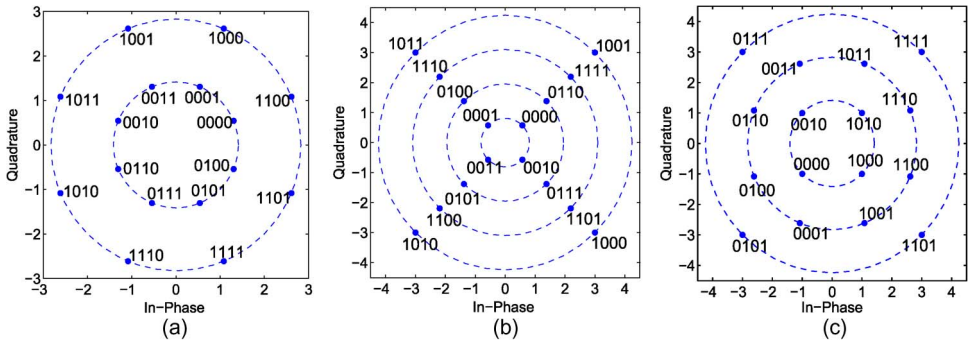

Fig. 1. Constellations of (a) (88)-APSK, (b) (4444)-APSK, and (c) (484)-APSK.

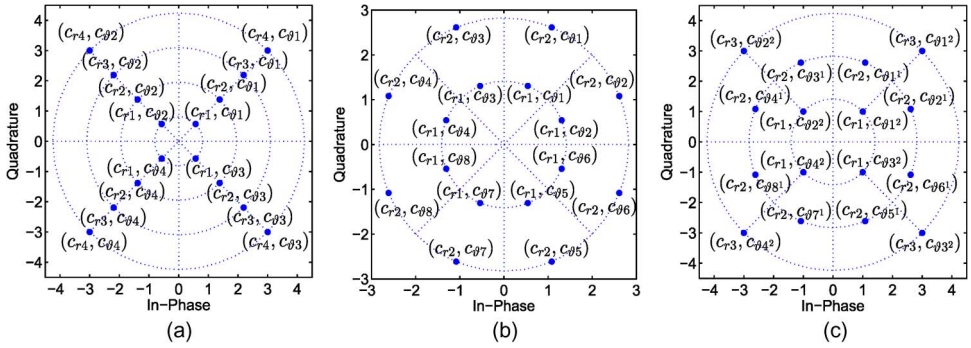

Fig. 2. Class assignment strategy of the amplitude and phase. $(c_{ri}, c_{\theta j})$ represents the ith class of the amplitude and jth class of the phase.

Choosing a good mapping scheme is crucial for APSK construction. Some distributions of APSK constellation are not applied to Gray mapping, which may lead to high demapping loss [16]. Accordingly, we set $\varphi = \varphi_k - \varphi_{k-1} = 0$, then the constellation which has a "rectangular" structure in polar coordinate can enable the application of Gray mapping. In order to gain better BER performance, we take the mapping scheme mentioned in [13] for 16-APSK constellation, which is developed from the Gray mapping for nonlinear channels: The labeled binary vectors of the kth ring is obtained from the Gray labeled constellation by a phase offset $(k-1) \times 2\pi / I_{k-1}$. Fig. 1 illustrates the three constellation distributions of 16-APSK formats which are used in our research. Notice that (484)-APSK is not the "rectangular" in polar coordinate, and it is labeled as the 16-QAM constellation.

3. Detection Scheme With SVMs

Based on the detection theory, the output symbols of optical fiber link, which are corrupted by the fiber NLPN, can be considered as groups of vectors and should match the transmitted signals with the best precision. Classification for the received signals as a kind of feasible detection way has been used to mitigate the NLPN [8]. The SVM is a useful technique for nonlinear data classification. At first each SVM split the clouds of data into two classes by the optimal binary classification hyperplane, which is obtained by solving its equivalent quadratic programming problem in the training process. Then under the established classification strategies, SVM conducts classification in the testing stage. The detailed principle of the SVM and the detailed derivation used for classification is shown in [8], [17], and [18].

In this section, we develop the scheme with SVMs for detecting the signal impaired by the NLPN in coherent 16-APSK optical systems. The detection scheme consists of two stages (TS): amplitude detection and phase detection. The class assignment strategies of the amplitude and phase in different distribution are shown in Fig. 2. For the sake of establishing the hyperplane of

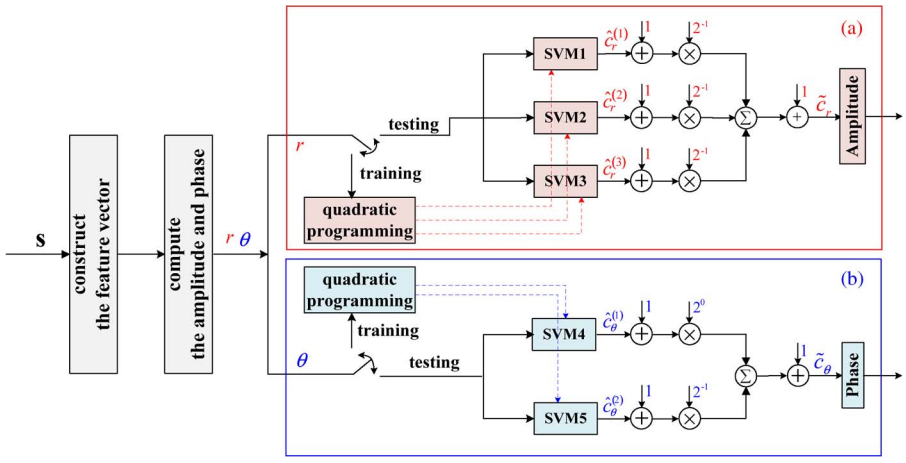

Fig. 3. Processing structure of the detector with SVMs for the (4444)-APSK system. A: amplitude detection. B: phase detection.

SVMs and detecting unknown symbols, we choose the in-phase and quadrature component of each received symbol as the elements of the feature vectors before training and testing stages. Then the detections are performed on amplitude and phase direction, respectively. The whole procedure of the TS detection scheme with SVMs is shown in Fig. 3 (e.g., (4444)-APSK).

3.1. Amplitude Detection

The vector $(r_1, r_2, \ldots, r_N)$ represents the radii distribution of the constellation. Obviously, we can divide the amplitudes into N classes, which can be labeled as $(c_{r1}, c_{r2}, \ldots, c_{rN})$. Each class representing the specific amplitude is labeled in binary format, and each bit is modeled by a conventional SVM. In order to distinguish the amplitude of the received signal, we need $N-1$ SVMs. In the training processing, the category information of training data can be obtained from the corresponding class label stored in the receiver. Then the binary classification strategy of the ith SVM for the training set can be given by

$$\begin{aligned} C_i^+ &= \{n \in S_r | n > i\} \\ C_i^- &= \{n \in S_r | n \le i\} \end{aligned} \tag{2}$$

where $S_r = \{1, 2, \ldots, N\}$ is the set of classes assigned to different amplitudes; n is the class label of training data; and C_i^+ and C_i^-, which satisfy $C_i^+ \cap C_i^- = 0$, $C_i^+ \cup C_i^- = S_r$, are the positive and negative class sets of the ith SVM, respectively. We label the training data as C_i^+ or C_i^- according to the principle of Eq. (2). For convenience, $\{+1, -1\}$ is used to represent $\{C_i^+, C_i^-\}$. Then the separating hyperplane of each SVM is obtained through the quadratic programming. Based on the established separating hyperplane, the received symbols in testing stage are classified by the ith SVM according to the discriminant function given as [8]

$$\hat{c}_r^{(i)} = \text{sign}\{L(\alpha)\} = \text{sign}\left\{\sum_{k=1}^{V} \alpha_k^{(i)} \cdot y_k^{(i)} \cdot \left\langle \mathbf{x}, \mathbf{x}_k^{(i)} \right\rangle + b_i\right\} \tag{3}$$

where $\mathbf{x}_k^{(i)}$, $\alpha_k^{(i)}$, b_i are the parameters of the quadratic programming, which are determined in the training process of ith SVM, $\mathbf{x}^{(i)}$ is the set of support vectors of the ith SVM, and V is the number of the support vectors of ith SVM. And each vector corresponds to a category label $y_k^i \in \{+1, -1\}$. $\mathbf{x}$ is the data to be detected. After $N-1$ times classification, we get $N-1$ bits. Then, the category of the amplitude is calculated by $\tilde{c}_r = 1 + \sum_{i=1}^{N-1} (\hat{c}_r^{(i)} + 1)/2$, and we can get the amplitudes of received symbols by the category $\tilde{c}_r$.

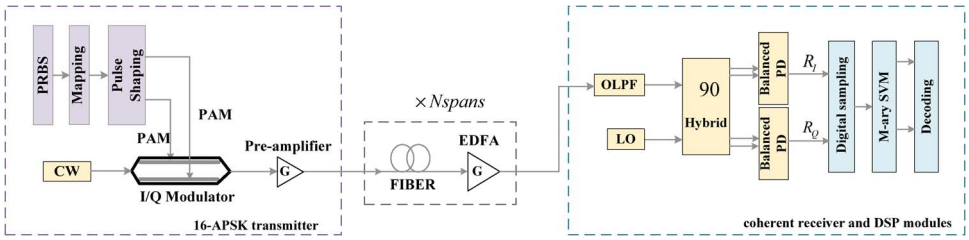

Fig. 4. Schematic diagram of the set-up used for simulations. PD: photodiode. LO: local oscillator.

3.2. Phase Detection

Similarly, we find that the phase distribution can also be divided into K classes which are labeled as $\{C_{\theta 1}, C_{\theta 2}, \ldots, C_{\theta K}\}$, as shown in Fig. 2. Only $\log_2 K$ SVMs are needed to classify the symbols in the phase direction. The binary classification strategy of the ith SVM is

$$C_i^+ = \left\{ n \in S_\theta | \bmod \left(\lceil n \cdot 2^{-(\log_2 K - i)} \rceil, 2 \right) = 0 \right\}$$
$$C_i^- = \left\{ n \in S_\theta | \bmod \left(\lceil n \cdot 2^{-(\log_2 K - i)} \rceil, 2 \right) \neq 0 \right\} \quad (4)$$

where $S_\theta = \{1, 2, \ldots, K\}$ represents the categories assigned to different phases, and K is the number of classes in the phase direction. Based on the established separating hyperplane, the ith SVM classifies the phase in the testing stage according to the discriminant function as (3), and then, the category of the phase can be calculated by

$$\tilde{c}_\theta = 1 + \sum_{i=1}^{\log_2 K} \left(\hat{c}_\theta^{(i)} + 1 \right) \cdot 2^{(\log_2 K - i - 1)}. \quad (5)$$

By now, we have obtained the amplitude and phase information of received signals. Subsequently, the received signals are demodulated into a binary sequence according to the encoding scheme. For example, if $(c_{r3}, c_{\theta 2})$ in (4444)-APSK is classified correctly by the SVMs, the $\hat{c}_r$ obtained by Eq. (3) is $\{\hat{c}_r^{(1)} = +1, \hat{c}_r^{(2)} = +1, \hat{c}_r^{(3)} = -1\}$, and $\hat{c}_\theta$ is $\{\hat{c}_\theta^{(1)} = -1, \hat{c}_\theta^{(2)} = +1\}$, So $\tilde{c}_r = 3$ and $\tilde{c}_\theta = 2$, then we get the corresponding binary sequence (1110) shown in Fig. 2.

Note that the (484)-APSK format has two kinds of phase distribution (i.e., 8 points per ring and 4 points per ring). In phase detection, the phases are firstly classified into $\tilde{c}_{\theta 1}$ in accordance with 8 points per ring. Based on the phase $\tilde{c}_{\theta 1}$, we get the phase $\tilde{c}_{\theta 2}$ accordingly. In other words, each point has two phases and subsequently which one to choose is depend on the amplitude in the decoding process.

4. Simulation Model and Results

4.1. Simulation Model

In this section, a set-up used for the numerical investigations by MATLAB is presented. And the schematic diagram of the set-up is shown in Fig. 4. For all numerical simulations, the baud rate is kept at 28 Gbaud resulting in the total bit rate of 112 Gb/s; the wavelength of the transmitter and LO laser is set to 1550 nm. In the transmitter, the length of the random binary sequence is 2^{18}; the I/Q modulator is driven by two pulse amplitude modulated (PAM) electrical signals, which are designed to generate the required 16-APSK constellations. The mappings in Fig. 1 for mapping four bits to a constellation point are used for the simulations. We learn from [19] that when the radii of the constellation are uniformly distributed, the system is highly immune to the nonlinear phase noise. So for simplicity, the radii of the ring constellations are set as (0.64, 1.28) $\sqrt{P_t}$, (0.48, 0.96, 1.44) $\sqrt{P_t}$ and (0.29, 0.70, 1.12, 1.54) $\sqrt{P_t}$, respectively.

In the fiber transmission subsystem, we first follow the model in [8], [10], and [11], in which we focus on the impacts of fiber NLPN and neglect the chromatic dispersion. The fiber link consists of $N \times 80$ km of dispersion shift fiber (DSF) with the nonlinear coefficient $\gamma = 1.3$ W^{-1}km^{-1} and the loss coefficient $\alpha = 0.2$ dB/km. EDFA is employed after each span, and the noise figure is set to be 5 dB. Then, we consider dispersion managed and unmanaged link. The dispersion managed link consists of N stages where each stage consists of 80 km of SSMF and the 17 km of DCF. The dispersion unmanaged link consists of N stages where each stage consists of 80 km of SSMF only. The parameters are as follows: $\alpha_{SMF} = 0.2$ dB/km, $\alpha_{DCF} = 0.5$ dB/km, $\gamma_{SMF} = 1.3$ W^{-1}km^{-1}, $\gamma_{DCF} = 5.3$ W^{-1}km^{-1}, and the dispersion parameter $D_{SMF} = 17$ ps/nm/km, $D_{DCF} = -80$ ps/nm/km. After the fiber transmission, the signals are coherently received in the receiver, converted to the electrical domain and sampled at the symbol rate $1/T$. We assume that the sampling frequency and the phase are synchronized to the incoming signal perfectly. Then the sampled signal is detected by the SVMs in amplitude and phase direction, respectively.

For all simulations, the LibSVM is adopted to conduct the model of SVMs in the detector, and 1000 symbols are used as training data to get the optimal hyperplane of each SVM. Besides, the RBF (radial basis function) is selected as the kernel function. The optimal value of the RBF kernel parameter σ and penalty factor C are obtained by the cross-validation procedure with grid-search approach [18]. In the simulation, the exact value $C = 0.5$ and $\sigma = 8$.

4.2. Results and Analysis

To evaluate the performances of SVMs for coherent optical 16-APSK systems, we compare the SVMs scheme (we denote it as TS-SVMs) with the TS detector proposed in [11] (we denote it as TS-ML). According to the TS-ML scheme, firstly the maximum likelihood (ML) radius detection is performed by mapping the amplitude of the received signals to one of the different amplitudes of the input signals. According to [20], the PDF of the amplitudes of the received signals is a Rice distribution, as shown in

$$f_{R|R_0=r_0}(r) = \frac{2r}{\sigma^2}\exp\left(-\frac{r^2+r_0^2}{\sigma^2}\right) I_0\left(\frac{2rr_0}{\sigma^2}\right) \tag{6}$$

where r and r_0 are the amplitudes of the received and transmitted symbols, respectively. σ^2 is the variance of ASE noise. I_0 is the modified Bessel function of the first kind. The values that define the mapping are given by the intersections of the Rice PDFs in (6)

$$f_{R|R_0=r_k}(\mu_k) = f_{R|R_0=r_{k+1}}(\mu_k). \tag{7}$$

We map R to r_k, when $\mu_{k-1} \le R \le \mu_k$. Based on the detected amplitude, a correction angle θ is calculated, which is given by [11]. Then, the ML detection is performed in the phase direction.

The received signals of different modulation formats in different launch powers and different fiber spans are processed by the TS-SVMs, TS-ML and direct decision, respectively. Firstly, we consider the DSF link. In Fig. 5, BER is plotted as a function of the input signal power for distance 1600 km. We can find that the performance is poor without the compensation of the NLPN. For the other two methods, the BER decreases with the growth of the transmitted power until the transmitted power reaches the optimal value, but as the launched power increases further, the BER increases again due to the dominance of NLPN. We can see clearly that by using the SVMs, the optimum launched power is increased with reduction in BER compared to the TS-ML. Fig. 5(a) shows the performance of the (88)-APSK system, from which we can learn that the TS-SVMs achieve a performance very close to that of the TS-ML at low launch power, while the BER performance of the system can be improved greatly with the use of SVMs at high transmitted powers. And by using SVMs, the system tolerance can be increased by 1.8 dB for BER $= 1E-3$ compared to the TS-ML. It is observed from Fig. 5(b) that the TS-SVMs has approximately 2.03 dB more launch power dynamic range than the TS-ML for BER $= 1E-3$ in the (484)-APSK system. Moreover, the performance of the (4444)-APSK system has been shown in

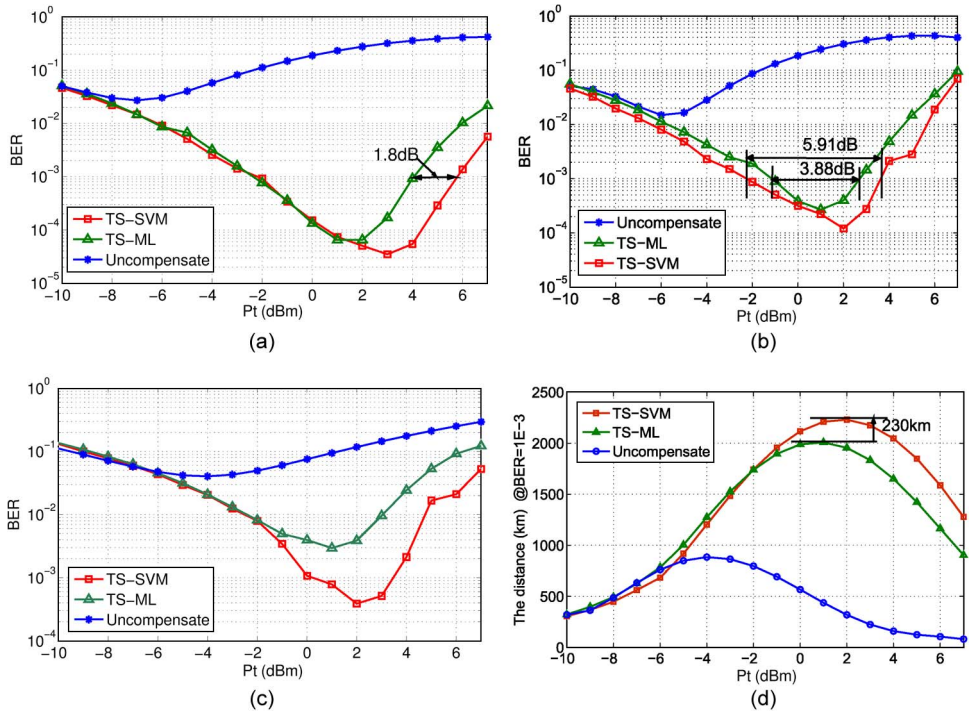

Fig. 5. Comparison between the TS-SVMs and TS-ML for different 16-APSK modulation formats. BER comparison of (a) (88)-APSK, (b) (484)-APSK, (c) (4444)-APSK, the transmission distance is 1600 km, and (d) maximum transmission distance of (88)-APSK for BER $= 1E-3$.

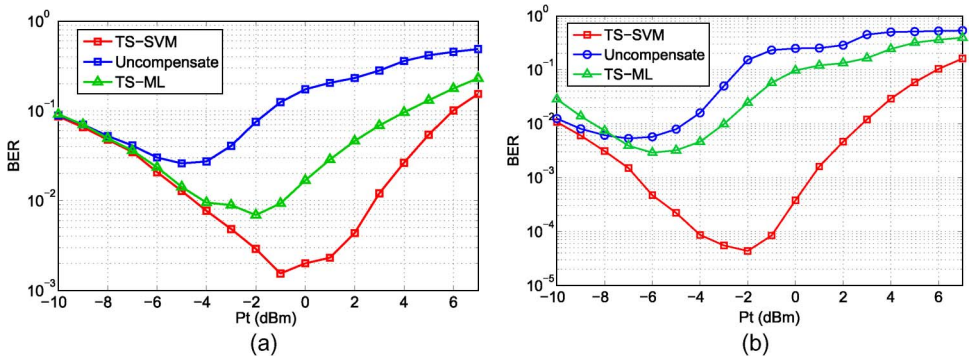

Fig. 6. BER comparison of (a) dispersion managed link and (b) dispersion unmanaged link.

Fig. 5(c). The optimal BER is $2E-3$ when TS-ML detection is used, while the BER gets down to $3E-4$ when the SVMs are applied. Since the (88)-APSK shows a better BER performance than other two constellations, Fig. 5(d) gives the comparison of the maximum distance as a function of input power in (88)-APSK system for BER $= 1E-3$. We can see that the optimal maximum distance is increased by 230 km when using the TS-SVMs detection, which means an improvement of 11.5% than using TS-ML detection.

Next, we consider dispersion managed link consisting of SSMF and DCF as described in Section 4.1. Since the (88)-APSK shows a better fiber nonlinearity tolerance than other constructed constellations, we choose it for this performance studies. In Fig. 6(a), BER is plotted as a function of the input signal power. The total number of spans is 12. It is observed from Fig. 6 (a) that a large improvement in the nonlinear system tolerance can be achieved when employing the TS-SVMs detection than the TS-ML. Then the DCF is removed and we consider 1200 km of

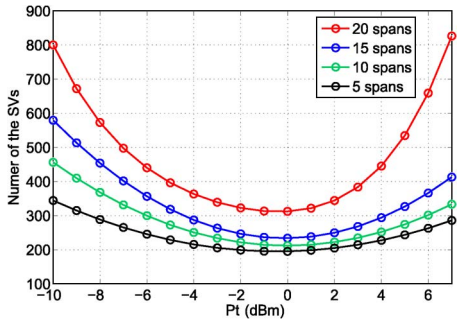

Fig. 7. Number of SVs in (88)-APSK.

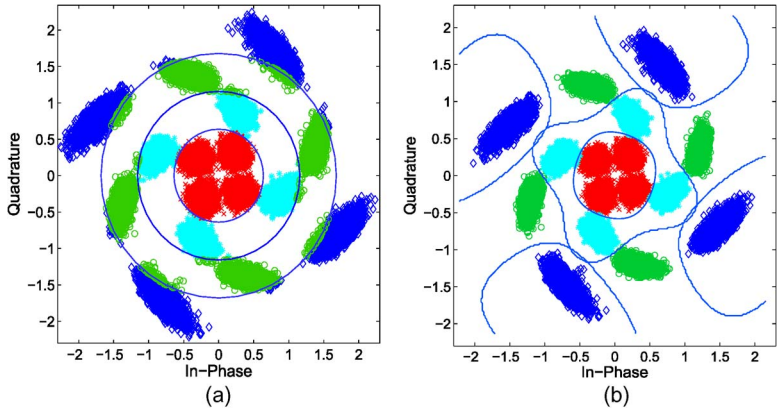

Fig. 8. Results of the detection by (a) TS-ML and (b)TS-SVMs for (4444)-APSK at $P_t = 2$ dBm; the DSF length is 1600 km. Different colors represent different amplitudes, and the curves represent the classification hyperplanes.

dispersion unmanaged signal transmission. The results of BER as a function of input power are shown in Fig. 6(b). We can learn that the performance of TS-ML is relatively poor. The reason for this is that the PDF of the received signal is Gaussian distribution rather than the Rice distribution when transmitting in the dispersion unmanaged link. It means the TS-ML would no longer suitable for this case. The result is in good agreement with the theory. While for the TS-SVM detection, a better performance of BER is achieved in dispersion unmanaged system. The reason why we get more improvement for the dispersion unmanaged link may be attributed to the fact that the effect of the nonlinearity corresponds to adding white Gaussian noise, which lead to some slight distortion in the shape of the clusters. While when transmitted in the dispersion managed link, the signals mix more seriously; therefore, a better performance can be achieved in classification with SVMs in dispersion unmanaged system.

Besides, we illustrate the number of support vectors (SVs) of (88)-APSK versus transmitted power for different DSF transmission distance in Fig. 7. The number of SVs can reflect the computational complexity of the TS-SVMs. We can observe that until the transmitted power reaches the optimal value, the complexity is high due to the ASE noise. And it declines rapidly with the increase of transmitted power. And the complexity increases with the further increasement of input power due to the heavy NLPN. What's more, the complexity is increased with the increase of the transmission distance.

The reason why we get more improvement for the TS-SVMs may be attributed to the advantages of the SVM as followings (e.g., (4444)-APSK):

1) In the amplitude direction, the TS-ML detector utilizes the theoretical PDF of the received amplitude to get the circular decision boundary μ_k. However, the decision boundaries are suboptimal as shown in Fig. 8(a). We can see that the optimal decision boundaries should

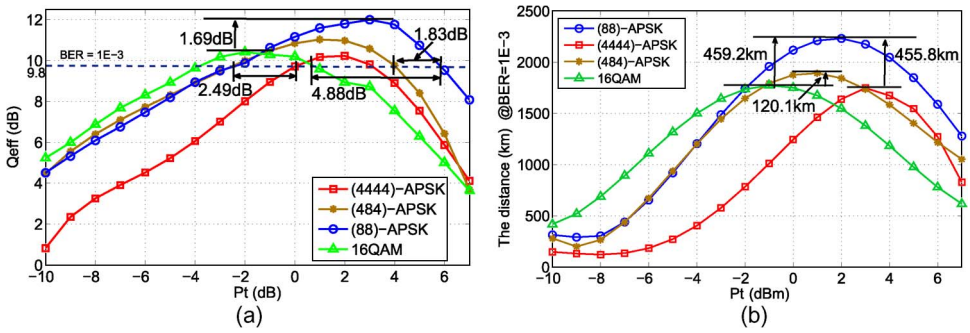

Fig. 9. Q-factor versus launch power; the DSF length is 1600 km. The dashed line represents the $Q_{eff} = 9.8$. (b) Maximum distance versus launch power for BER $= 1E-3$.

no longer be round when the NLPN dominates. Fig. 8(b) shows the result of the detection in amplitude direction by SVMs. Compared with the TS-ML detector, the SVMs get the optimal decision hyperplane based on the specific distribution of received signal.

2) In TS-ML detector, the phase rotation is performed on the basis of the mapped amplitude. In other words, the error in the amplitude detection may lead directly to the error in the phase detection. While by using SVMs, the phase detection is performed directly without the phase rotation step. It means that the detections in amplitude and phase direction are separated and irrelevant.
3) The TS-ML have requirement on the transmission link, while the detection with TS-SVMs is suitable for any transmission link.

Furthermore, the performance comparison between the three 16-APSK constellations and the square 16-QAM when using the TS-SVMs detection are given. We plot Q_{eff} as a function of input power after 1600 km transmission DSF link in Fig. 9(a). As expected, the 16-QAM outperforms 16-APSK constellations in the low launch powers less than -2 dBm, while the 16-APSK constellations show a significant performance improvement in the high launch powers. And the improvement of the nonlinear tolerance depends on the modulation formats. When using the (88)-APSK, we can observe an improvement of up to 4.88 dB in nonlinear tolerance compared to the square 16-QAM for BER $= 1E-3$, and an improvement of 1.83 dB compared to the (484)-APSK. Moreover, the optimal Q-factor of the (88)-APSK system is higher than that of the 16-QAM by 1.69 dB.

Besides, the (484)-APSK can gain an improvement of the nonlinear tolerance by 2.49 dB for BER $= 1E-3$ over the (4444)-APSK system. The results of the maximum transmission distance as a function of input power for BER $= 1E-3$ in systems with different modulation formats are shown in Fig. 9(b). It is observed that the achievable maximum transmission distance of the (4444)-APSK is approximately as same as 16-QAM. Compared to the achievable maximum distance of 16-QAM, the distance of the (484)-APSK and (88)-APSK is increased by 120.1 km and 459.2 km. In other words, the maximum reach improvement of the (88)-, (484)-, and (4444)-APSK is 25.9%, 6.7%, and 0.19% compared to 16-QAM, respectively.

5. Conclusion

In this paper, we have introduced a new detection scheme with SVMs for coherent optical 16-APSK systems. It is a powerful tool for mitigating the nonlinear phase noise without requiring the characteristics of the fiber link. In order to investigate the performance of SVMs, we conduct numerical simulations for 112 Gb/s single channel 16-APSK with three modulation formats (4444-, 88-, 484-) APSK systems respectively. Three kinds of transmission link are considered, namely DSF, SSMF and DCF, SSMF only. The numerical results show that the SVMs allow higher transmitter powers to be used. It can achieve a relatively large improvement in nonlinear system tolerance compared with the suboptimal TS detector with ML for all listed 16-APSK

constellations. Especially for the (88)-APSK system, an improvement of 1.8 dB in nonlinear tolerance and 11.5 % in maximum distance are obtained for systems in which the signals are mainly deteriorated by the nonlinear phase noise. Besides, the results have illustrated that the TS-SVMs detection has good performance for any transmission link. Additionally, we have demonstrated that the 16-APSK modulation formats are more appropriate for the high nonlinear regimes than the 16-QAM constellation. When using the (88)-APSK modulation format, the increased nonlinear phase tolerance can be 4.88 dB compared to the 16-QAM constellation. The performance investigation and improvement of APSK systems with the SVMs for the practical systems with 16-points or higher order constellations need to be investigated in the future.

References

[1] E. Ip, A. Pak, D. Barros, and J. M. Kahn, "Coherent detection in optical fiber systems," *Opt. Exp.*, vol. 16, no. 2, pp. 753–763, Jan. 2008.

[2] J. M. Kahn and K.-P. Ho, "Spectral efficiency limits and modulation/detection techniques for DWDM systems," *IEEE J. Sel. Topics Quantum Electron.*, vol. 10, no. 2, pp. 259–271, Mar./Apr. 2004.

[3] R.-J. Essiambre, G. Kramer, P. J. Winzer, G. J. Foschini, and B. Goebel, "Capacity limits of optical fiber networks," *J. Lightw. Technol.*, vol. 28, no. 4, pp. 662–701, Feb. 2010.

[4] K. Roberts, C. Li, L. Strawczynski, M. O'Sullivan, and I. Hardcastle, "Electronic precompensation of optical nonlinearity," *IEEE Photon. Technol. Lett.*, vol. 18, no. 2, pp. 403–405, Jan. 2006.

[5] K.-P. Ho and J. M. Kahn, "Electronic compensation technique to mitigate nonlinear phase noise," *J. Lightw. Technol.*, vol. 22, no. 3, pp. 779–783, Mar. 2004.

[6] A. S. Tan *et al.*, "An ML-based detector for optical communication in the presence of nonlinear phase noise," in *Proc. IEEE Int. Conf. Commun.*, 2011, pp. 1–5.

[7] Z. Xu, B. Zhang, P. Y. Kam, and C. Yu, "Adaptive maximum likelihood sequence detection in 100-Gb/s coherent optical communication system," in *Proc. OFC/NFOEC*, 2013, pp. 1–3.

[8] M. Li *et al.*, "Nonparameter nonlinear phase noise mitigation by using m-ary support vector machine for coherent optical systems," *IEEE Photon. J.*, vol. 5, no. 6, p. 7800312, Dec. 2013.

[9] M. Seimetz, *High-Order Modulation for Optical Fiber Transmission*. Berlin, Germany: Springer-Verlag, 2009.

[10] C. Hager, A. Graell i Amat, A. Alvarado, and E. Agrell, "Constellation optimization for coherent optical channels distorted by nonlinear phase noise," in *Proc. IEEE GLOBECOM*, Anaheim, CA, USA, Dec. 2012, pp. 2870–2875.

[11] A. P. T. Lau and J. M. Kahn, "Signal design and detection in presence of nonlinear phase noise," *J. Lightw. Technol.*, vol. 25, no. 10, pp. 3008–3016, Oct. 2007.

[12] L. Beygi, E. Agrell, and M. Karlsson, "Optimization of 16-point ring constellations in the presence of nonlinear phase noise," presented at the Optical Fiber Communication Conf., Los Angeles, CA, USA, Paper OThO4.

[13] C. Hger, A. Graell i Amat, and E. Agrell, "Design of APSK constellations for coherent optical channels with nonlinear phase noise," *IEEE Trans. Commun.*, vol. 61, no. 8, pp. 3362–3373, Aug. 2013.

[14] L. Beygi, E. Agrell, P. Johannisson, and M. Karlsson, "A novel multilevel coded modulation scheme for fiber optical channel with nonlinear phase noise," in *Proc. IEEE Global Commun. Conf.*, 2010, pp. 1–6.

[15] R. D. Gaudenzi, S. Member, A. G. Fabregas, and A. Martinez, "Performance analysis of turbo-coded APSK modulations over nonlinear satellite channels," *IEEE Trans. Wireless Commun.*, vol. 5, no. 9, pp. 2396–2407, Sep. 2006.

[16] Z. Liu, Q. Xie, K. Peng, and Z. Yang, "APSK constellation with Gray mapping," *IEEE Commun. Lett.*, vol. 15, no. 12, pp. 1271–1273, Dec. 2011.

[17] V. N. Vapnik, *The Nature of Statistical Learning Theory*. Berlin, Germany: Springer-Verlag, 1995.

[18] C. W. Hsu, C. C. Chang, and C. J. Lin, *A Practical Guide to Support Vector Classification*, 2008. [Online]. Available: http://www.csie.ntu.edu.tw/~cjlin/papers/guide/guide.pdf

[19] M. C. Niaz and L. Beygi, "Optimization of 16-QAM constellation in the presence of nonlinear phase noise," in *Proc. Int. Conf. Frontiers Inf. Technol.*, Islamabad, Pakistan, Dec. 2009, pp. 62.

[20] K.-P. Ho, *Phase-Modulated Optical Communication Systems*. New York, NY, USA: Springer-Verlag, 2005.